Journal of Hazardous Materials 201–202 (2012) 100–106

Contents lists available at SciVerse ScienceDirect

Journal of Hazardous Materials

journal homepage: www.elsevier.com/locate/jhazmat

Degradation of Acid Red 274 using H_2O_2 in subcritical water: Application of response surface methodology

Berkant Kayan[a,*], Belgin Gözmen[b]

[a] Department of Chemistry, Arts and Sciences Faculty, Aksaray University, Aksaray, Turkey
[b] Department of Chemistry, Arts and Sciences Faculty, Mersin University, Mersin, Turkey

ARTICLE INFO

Article history:
Received 12 September 2011
Received in revised form 31 October 2011
Accepted 13 November 2011
Available online 20 November 2011

Keywords:
Degradation
Response surface methodology
Box–Behnken design
Subcritical water

ABSTRACT

In this research, the degradation of Acid Red 274 (AR 274) was investigated under subcritical water conditions using H_2O_2, which led to the oxidative degradation of Acid Red 274 up to its 80% of mineralization. The Box–Behnken design matrix and response surface methodology (RSM) were applied in designing the experiments for evaluating the interactive effects of the three most important operating variables. Thus, the interactive effects of temperature (100–250 °C), oxidant (H_2O_2) concentration (50–250 mM), and time (30–60 min.) on the degradation of AR 274 were investigated. A total of 17 experiments were conducted in this research, and the analysis of variance (ANOVA) indicated that the proposed quadratic model could be used for navigating the design space. The proposed model was essentially in accordance with the experimental case with correlation coefficient $R^2 = 0.9930$ and Adj-$R^2 = 0.9839$, respectively.

The results confirmed that RSM based on the Box–Behnken design was a compatible method for optimizing the operating conditions of AR 274 degradation.

Nomenclature

AR 274	Acid Red 274
AOPs	Advanced oxidation processes
RSM	Response surface methodology
BBD	Box–Behnken design
SW	Subcritical water
DE	Degradation efficiency
TOC	Total organic carbon
C_t	Dye concentration at any time (mg/L)
C_0	Initial dye concentration (mg/L)
ANOVA	Analysis of variance

1. Introduction

The textile industry is very water intensive. Water is used for cleaning the raw material and in several flushing steps throughout production. Textile wastewaters are comprised of a variety of dyes and chemicals that make the chemical composition of textile industry effluents an environmental challenge. Most of the pollution in textile wastewater is a result of dyeing and ending processes [1,2].

Textile wastewaters contain various organic pollutants that are dissolved in water depending on the kind of dyeing solution used [3]. At present, more than 100,000 different dyes are commercially produced and synthesized on an industrial scale, which are commonly used in textile, paper, and other industries. Typically, these types of dyes can be classified according to the chemical structures of their particular chromophoric group. One of the dyes widely used in textile industries are acid dyes [4]. Nearly 30 million tons of dyes have been produced in the world in recent years. The growth rate is increasing gradually and this increasing production rate is reflected directly or indirectly in environmental pollution [5,6]. As a result, wastewaters produced by the textile industries include remarkable amounts of non-fixed dyes, especially azo dyes containing one or more nitrogen to nitrogen double bonds (–N=N–). Azo dyes constitute a significant portion of dyes that are used in industries nowadays. The products of degradation could be mutagenic and carcinogenic, thereby causing long-term health concern [7,8]. Thus, the treatment of the effluents containing such compounds is important for the protection of natural waters as well as the environment. The conventional treatments of wastewaters containing organic compounds include biological oxidation, chemical coagulation, advanced oxidation (AOPs), and adsorption [9–11]. On the other hand, the use of subcritical water, with or without oxidants is an effective method for the degradation of potential pollutants in water environment [12]. In addition, under the subcritical state,

* Corresponding author. Tel.: +90 0382 2882143; fax: +90 0382 2882125.
E-mail addresses: berkantkayan@aksaray.edu.tr, berkantkayan@gmail.com (B. Kayan).

0304-3894/$ – see front matter © 2011 Elsevier B.V. All rights reserved.
doi:10.1016/j.jhazmat.2011.11.045

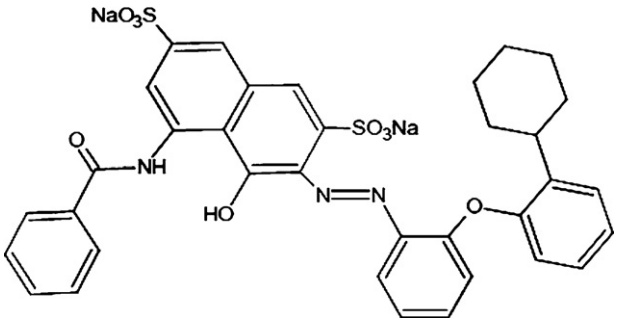

Fig. 1. Molecular structure of reactive Acid Red 274 dye.

the concentrations of H^+ and OH^- are appropriately increased via self-ionization of water molecules. However, the combination of subcritical water with oxidizing agents such as hydrogen peroxide, permanganate, and oxygen, etc. can efficiently oxidize various compounds that are otherwise very difficult to oxidize. Therefore, in recent years, some approaches have been designed to use subcritical water for the degradation of hazardous compounds [13–20]. In this research work, the aqueous solution of AR 274 was selected as a model for textile wastewaters for evaluation under subcritical water conditions. In another part of this study, response surface methodology (RSM) was used to find an applicable approximating function for predicting and determining the further response as well as studying the optimum working state [21].

Response surface methodology (RSM) is an effective instrument for optimizing the process when a combination of a few independent variables and their interactions affects requests and responses [22,23].

To our knowledge, there has been no study conducted until now for the optimization of parameters using RSM based on the Box–Benhken design (BBD) in azo dye degradation by subcritical water in the presence of H_2O_2.

2. Materials and methods

2.1. Materials

The azo dye C.I. Acid Red 274, commercial name Supranol Red 3BW, was supplied by Dystar (Germany) and was used without further purification. The solution of AR 274 was prepared in 1000 mg/L initial concentration with distilled water for all the treatments. Its chemical structure is depicted in Fig. 1. Hydrogen peroxide (Merck) was used for the oxidant subcritical water process.

2.2. Subcritical water system and process

The experimental process is described in detail in Yang et al. [24,25]. A brief overview of the process is as follows: stainless steel vessels (7.07 mL with 9 cm × 1 cm I.D.) were used for the degradation process. Both ends of the vessels were wrapped with two layers of Teflon tape and one end was tightly sealed with an end cap. Each vessel was loaded with 5 ml dye solution, and 35% H_2O_2 (w/v) was added to the vessels and capped. The experiments were performed in triplicate for all reaction conditions. Vessels were placed in a Shimadzu GC-9A oven for heating. All experiments were performed in a temperature range of 100–250 °C for 30, 45, and 60 min. Subsequent to the desired reaction time, the vessels were removed from the oven and allowed to cool at room temperature.

2.3. Analysis

In this research, AR 274 dye concentration was analyzed spectrophotometrically on a UV–vis spectrometer (Shimadzu UV-160A) at 527 nm by measuring the absorbance of the untreated samples at maximum wavelength. The percentage of AR 274 degradation efficiency (DE%) was calculated using the following formula:

$$\text{DE } (\%) = \frac{C_o - C_t}{C_o} \times 100 \quad (1)$$

where C_o and C_t represent the initial and remaining AR 274 concentrations at given time t, respectively.

The mineralization of AR 274 solution was monitored by the reduction of the total organic carbon (TOC), which was measured on a Tekmar-Dorhmann Apollo 9000 TOC analyzer.

The GC–MS analysis was performed using the 5890A Agilent model gas chromatograph, interfaced with the ECD, NPD, and 5975C mass selective detector. The aqueous solutions were extracted three times with 15 mL dichloromethane. A 3 μL sample was analyzed on GC–MS. An HP5-MS capillary column (30 m × 0.25 mm × 0.25 μm) was used as the analytical column. Helium was used as the carrier gas with a flow rate of 2 mL/min. The GC injection port temperature was set at 250 °C (split mode = 1/5), and the column temperature was fixed at 70 °C for 5 min. Subsequently, the column was sequentially heated at a rate of 5 °C/min to 120 °C and held for 1 min, at a rate of 8 °C/min to 200 °C and held for 5 min, and at a rate of 10 °C/min to 280 °C and held for 10 min. The MS detector was operated in the EI mode (70 eV).

2.4. Experimental design and optimization

In the present study, response surface methodology (RSM) is used for the optimization of process variable to enhance the degradation of AR 274 dye combined with Box–Behnken design. In recent years, RSM has been used in various fields of science, and its feasibility and efficiency have been highlighted by several research groups [22]. A comparison was made between the Box–Behnken design and other response surface designs (central composite, Doehlert matrix, and three-level full factorial designs) and it was observed that the Box–Behnken and Doehlert matrix designs are notably less effective than the central composite design but considerably more effective than the three-level full factorial designs [26,27].

The Box–Behnken design is a free, spherical and rotatable quadratic design, which consists of a central point and the midpoints of the edges of the cube restricted on the area. Furthermore, the Box–Behnken design suffers calculations of the response function at intermediate levels and makes it possible to guess the system performance at any experimental point in the range studied owing to the careful design and analysis of experiments [28–30].

In this study, the three levels, three-factorial Box–Behnken experimental design was applied for investigating and validating the process parameters that affect the removal of textile dye AR 274 under the SW process [31]. The three critical parameters affecting AR 274 degradation, namely temperature (x_1), H_2O_2 concentration (x_2), and experimental time (x_3), were selected as independent variables based on preliminary experiments, and removal TOC% (Y) was considered as the dependent variable (response). The experimental range and levels of independent variables for AR 274 degradation are given in Table 1 [32]. The experimental results were analyzed using Design Expert 8.1 (trial version) and the regression model was proposed.

In the optimization process, the responses can be simply related to the chosen factors by linear or quadratic models. A quadratic model, which also includes the linear model, is given below as Eq.

Table 1
Experimental range and levels of the independent variables.

Variables	Factor	Range and level		
		−1	0	1
Temperature (°C)	X_1	100	175	250
H_2O_2 (mM)	X_2	50	150	250
Time (min)	X_3	30	45	60

(2)

$$Y = \beta_o + \beta_1 x_1 + \beta_2 x_2 + \beta_3 x_3 + \beta_{12} x_1 x_2 + \beta_{13} x_1 x_3 + \beta_{23} x_2 x_3 + \beta_{11} x_1^2 + \beta_{22} x_2^2 + \beta_{33} x_3^2 + \varepsilon \quad (2)$$

where Y is the response and x_1, x_2, and x_3 represent the effect of the independent variables. Thus, x_1^2, x_2^2, x_3^2 are the square effects, and x_1x_2, x_1x_3, and x_2x_3 are the interaction effects; β_1, β_2, and β_3 are the linear coefficients, and β_{12}, β_{13}, β_{23} are the interaction coefficients. β_o and ε represent the constant and the random error, respectively [32].

In this study, a total of 17 experiments were performed in randomized order as required in many design procedures. The adequacy of the proposed model is then revealed using the diagnostic checking tests provided by analysis of variance (ANOVA). The property of the fit polynomial model is represented by the coefficient of determination R^2. The R^2 values assure a measure of how variability in the observed response values can be clarified by experimental factors and their interactions. These analyses are performed by the agency of Fisher's 'F' test and P-value (probability) [33]. Based on the experimental data obtained, the levels of the three main parameters investigated in this study are presented in Table 1. For statistical calculations, the variables X_i (the real value of an independent variable) were coded as x_i (dimensionless value of independent variable) according to the following equation:

$$X_i = \frac{X_i - X_o}{\delta X} \quad (3)$$

where X_o is the value of X_i at the center point, and δX represents the step change [33].

3. Result and discussion

3.1. Optimization of degradation conditions using RSM approach

Response surface methodology was employed for identifying the simple and interactive effects of the operating variables of AR 274 degradation for the SW process. According to the RSM results, polynomial regression modeling was operated between the responses of the corresponding coded values of the three different process variables, and finally, the best model equation was obtained as follows [34]:

$$Y = 54.70 + 26.78X_1 + 4.51X_2 - 0.54X_3 - 1.98X_1X_2 + 4.38X_1X_3 - 1.15X_2X_3 - 2.72X_1^2 - 8.70X_2^2 - 2.10X_3^2 \quad (4)$$

Statistical approaches with a Box–Behnken design were used for efficient degradation of Acid Red 274 and for determining the interaction between these factors. For the response surface methodology involving Box–Behnken design, a total of 17 experiments were conducted for three factors at three levels. Table 1 provides a list of independent variables and coded factor levels. An RSM is appropriate when the optimal region for running the process has been identified. The design used for the optimization and the responses observed for the 17 experiments are depicted in Table 2. In Eq. (4), Y is the TOC removal percent of AR 274, and x_1, x_2, and x_3 are the corresponding coded variables of temperature, H_2O_2 concentration, and time.

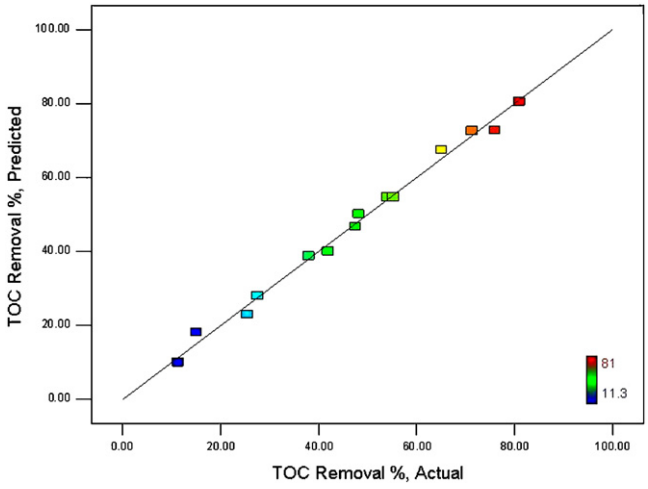

Fig. 2. The actual and predicted TOC removal %.

3.2. Analysis of variance (ANOVA)

The analysis of variance (ANOVA) results of quadratic models are shown in Table 3 for the SW process. The model's F-value of 109.77 implies that the model is significant for the degradation of AR 274. Adequate precision measures the signal to noise ratio, and a ratio value greater than 4 is desirable. Therefore, in the quadratic model degradation of dye, an adequate precision of 36.12 indicates an adequate signal for the SW process. P-values less than 0.05 indicate that the model terms are significant, whereas values greater than 0.1 are not significant. The fit of the models was controlled by the coefficient of determination R^2. Based on the ANOVA results, the models report high R^2-value of 99.30%. Also, an acceptable agreement with the adjusted determination coefficient is necessary. In this study, the adjusted R^2-value was found to be 98.39%. The value of R^2 and adjusted R^2 is close to 1.0, which is considerably high, thus advocating a high correlation between the observed values and the predicted values. This indicates that the regression model provides an excellent explanation of the relationship between the independent variables and the responses [22,32,35–37]. The diagnostic plot shown in Fig. 2 was used for estimating the adequacy of the regression model.

The actual and the predicted TOC removal % values are depicted in Fig. 3. It is observed that there are tendencies in the linear regression fit, and the model adequately explains the experimental range studied. The actual TOC removal % value is the measured result for a specific run and the predicted value is evaluated from the independent variables in the BBD [32]. The normal % probability and studentized residuals plot is shown in Fig. 4. The data points indicate that neither response transformation was needed nor any apparent problem with normality was present.

3.3. Interactive effect of process independent variables

To understand the impact of each variable, three dimensional (3D) plots were made for the estimated responses, which were the bases of the model polynomial function for analysis, to investigate the interactive effect of two factors on the TOC removal % within the experimental ranges given in Fig. 5. The inferences so attained are discussed below [38].

Table 2
Box–Behnken design experiments and experimental results.

Experiment number	Experimental design			Experimental plan			Observed%Y	Predicted %Y
	T (°C)	H_2O_2 (mM)	t (min)	X_1	X_2	X_3		
1	−1	−1	0	100	50	45	11.30	10.01
2	+1	−1	0	250	50	45	65.10	67.51
3	−1	+1	0	100	250	45	25.40	22.99
4	+1	+1	0	250	250	45	71.30	72.59
5	−1	0	+1	100	150	60	27.50	28.01
6	+1	0	−1	250	150	30	76	72.81
7	−1	0	−1	100	150	60	15	18.19
8	+1	0	+1	250	150	60	81	80.49
9	0	−1	−1	175	50	30	38	38.78
10	0	+1	−1	174	250	30	48.20	50.10
11	0	−1	+1	175	50	60	41.90	40
12	0	+1	+1	175	250	60	47.50	46.73
13	0	0	0	175	150	45	54.60	54.70
14	0	0	0	175	150	45	54.50	54.70
15	0	0	0	175	150	45	55.10	54.70
16	0	0	0	175	150	45	54.0	54.70
17	0	0	0	175	150	45	55.30	54.70

Table 3
Analysis of variance regression model for AR 274 degradation by using SW process.

Source	Degrees of freedom	Sum of squares	Mean square	*F*-value	*P*-value
Model	9	6391.02	710.11	109.77	<0.0001
X_1	1	5735.21	5735.21	*886.58*	<0.0001
X_2	1	162.90	162.90	25.18	0.0015
X_3	1	2.31	2.31	0.36	0.5688
X_1^2	1	31.27	31.27	4.83	0.0639
X_2^2	1	318.69	318.69	49.27	0.0002
X_3^2	1	18.57	18.57	2.87	0.1340
X_1X_2	1	15.60	15.60	2.41	0.1644
X_1X_3	1	76.56	76.56	11.84	0.0108
X_2X_3	1	5.29	5.29	0.82	0.3959
Residual	7	45.28	6.47		
Lack of fit	3	44.22	14.74	55.63	0.0010
Pure error	4	1.06	0.27		

R^2 = 0.9930, R^2_{Adj} = 0.9839, CV% = 5.26, adequate precision = 36.128.

3.3.1. *Interactive effect of temperature and oxidant concentration*

To investigate the integrated effect of temperature and oxidant concentration, the RSM was used and the result was shown in the form of three dimensional (3D) plots. As indicated in Fig. 5, with an increase in the oxidant concentration, the TOC removal % increased with temperature until it reached the optimum grade. The removal % of AR 274 increased with rising temperature for the SW process. For example, in Fig. 5 (at 50 mM H_2O_2, temperature 100 °C) the TOC removal % was 11.30%, which increased to 54.60% at 150 mM H_2O_2 and temperature 175 °C when the SW process was used. Fig. 5 demonstrates that the TOC removal % efficiency increased with an increase in the concentration of hydrogen peroxide; however, once it exceeded a definite grade, it was pioneered by a decrease in the degradation rate. This might be possible because as the concentration of hydrogen peroxide is increased, more OH• radicals are

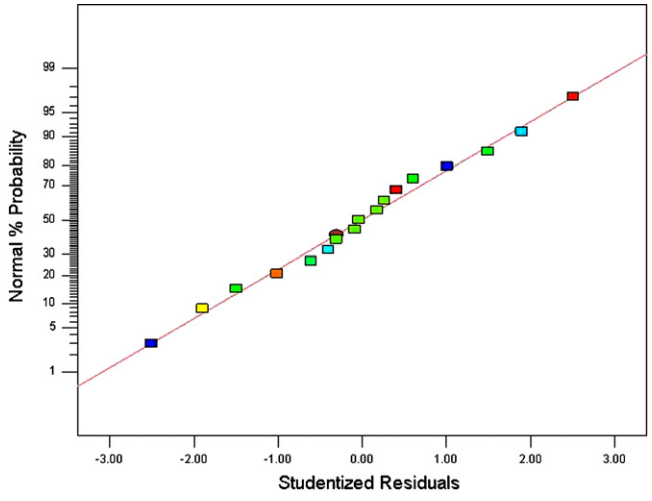

Fig. 3. The studentized residuals and normal % probability plot of degradation of AR 274.

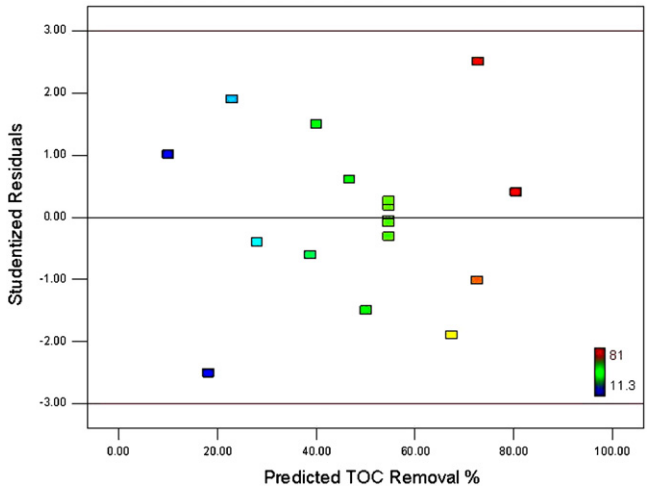

Fig. 4. The predicted TOC removal % of AR 274 and studentized residuals plot.

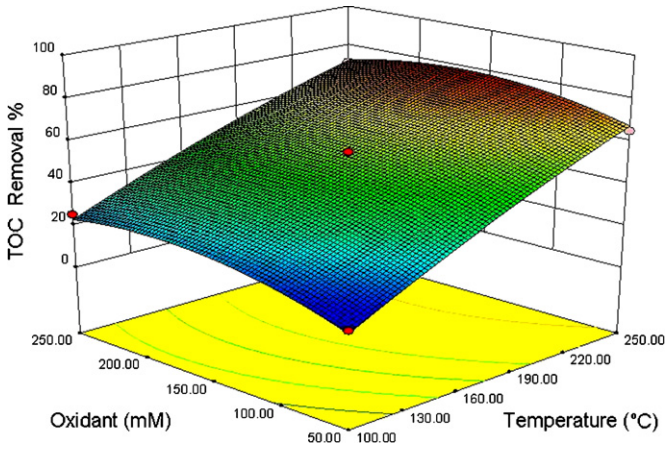

Fig. 5. Surface and contour plots of TOC removal versus experiment temperature (°C) and oxidant (H_2O_2) concentration (mM) at a fixed reaction time t = 45 min.

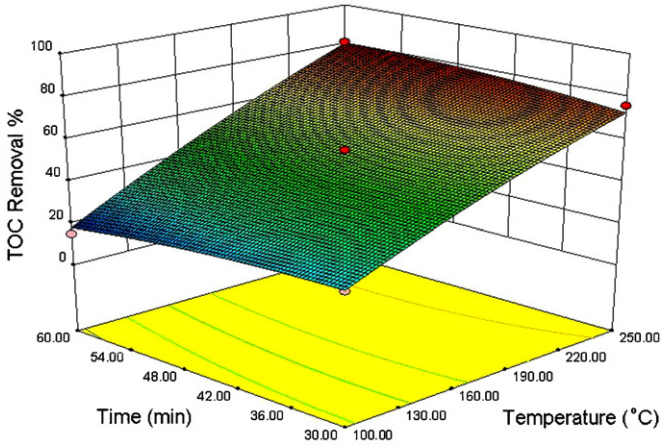

Fig. 6. Surface and contour plots of TOC removal versus experiment temperature (°C) and experiment time (min) at a fixed oxidant concentration [H_2O_2] = 150 mM.

ready to attack the dye and the rate of degradation reaction thus increases. However, the hydroxyl free radicals finally reach equilibrium with hydrogen peroxide, and at this point, hydrogen peroxide is used considerably more; the OH• radical effectively reacts with hydrogen peroxide and produces hydroperoxide (HO_2•). As already known, hydroperoxide radicals are less reactive than OH• radicals, which explains the reason for the decrease in the degradation reaction. The reactions involved are as follows: [38–40]

$$H_2O_2 + {}^{\bullet}OH \rightarrow HO_2{}^{\bullet} + H_2O \quad (5)$$

$$H_2O_2 + {}^{\bullet}OH \rightarrow O_2{}^{\bullet -} + H^+ + H_2O \quad (6)$$

$${}^{\bullet}OH + {}^{\bullet}OH \rightarrow H_2O_2 \quad (7)$$

$${}^{\bullet}OH + HO_2{}^{\bullet} \rightarrow H_2O + O_2 \quad (8)$$

In addition to hydroxyl radicals generated at high concentration dimerize to hydrogen peroxide, it is indicated in Eq. (7).At subcritical water conditions, H_2O_2 decomposes to produce very reactive OH• radicals according to the reaction given below:

$$H_2O_2 \rightarrow 2OH^{\bullet} \quad (9)$$

As the life span of hydroxyl radicals is very limited, they can react only where they occur [39]. Thus, the degradation rate is affected by H_2O_2 concentration and experimental temperature. It was found that the decomposition rate of hydrogen peroxide increased with rising experimental temperature and caused H_2O_2 to decompose very rapidly to the OH• radicals. Finally, the OH• radicals formed could rapidly attack the dye molecule, thereby pioneering its degradation. Fig. 8 depicts the proposed degradation mechanism for AR 274 at subcritical water conditions using H_2O_2 as the oxidant [12].

3.3.2. Interactive effect of temperature and time

Fig. 6 presents 3D plots demonstrating the effect of temperature and time on percentage TOC removal under the predefined conditions specified by Design Expert. It is seen in Fig. 6 that the maximum 81.0% TOC removal occurs at the 60 min of experimental time and at 250 °C in SW conditions. The degradation rate increases with an increase in the experimental time at lower temperature; however, when the temperature increases, the effect of time becomes limited and temperature becomes the dominant factor owing to the interaction between oxidant and temperature. Thus, the degradation rate is particularly controlled by the temperature as detailed above, whereas time is probably less important for the degradation rate of dye.

3.3.3. Interactive effect of oxidant and time

In Fig. 7, the response surface and three dimensional plots were developed as a function of oxidant concentration and experimental time. As seen in Fig. 7, the TOC removal % rate increases with increased time and oxidant concentration at constant temperature. With increasing experimental time, the probability of interactions of radicals with the dye also increases. However, regardless of the experimental time, this interaction will be limited to the amount of the radical formed.

3.4. Identification of products

Fig. 8 depicts the GC–MS analysis of short-time oxidized solutions in subcritical water condition revealing the formation of bezamide [m/e = 121 (68, M^+)], benzoic acid [m/e = 122 (81, M^+)], hydroquinone [m/e = 110 (100, M^+)], benzoquinone [m/e = 108 (100, M^+)], 1-naphthol [m/e = 144 (100, M^+)], phtalic anhydride [m/e = 148 (43, M^+)], phthalic acid [m/e = 166 (13, M^+)], and o-cyclohexylphenol [m/e = 176 (89, M^+)]. Based on these findings, a possible degradation pathway for AR 274 is illustrated in Fig. 8. In the process, C(3)-N, C(5)-N, and C(20)-O bonds were cleavaged owing to temperature effects and attacks of hydroxyl radicals. Through the cleavage of C(5)-N bond, bezamide (**A1**) was separated from dye structure and was then converted to benzoic acid (**A2**), hydroquinone (**A3**), and benzoquinone (**A4**) owing to further attacks of OH· radicals. The cleavage of the C(5)–N and C(3)–N bonds

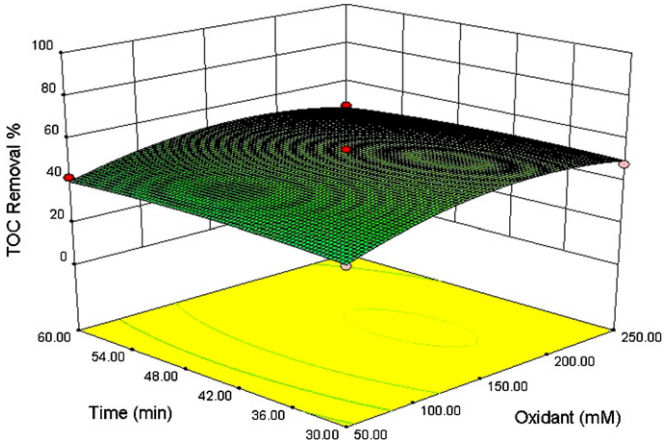

Fig. 7. Surface and contour plots of TOC removal versus oxidant (H_2O_2) concentration (mM) and experiment time (min) at a fixed temperature T = 175 °C.

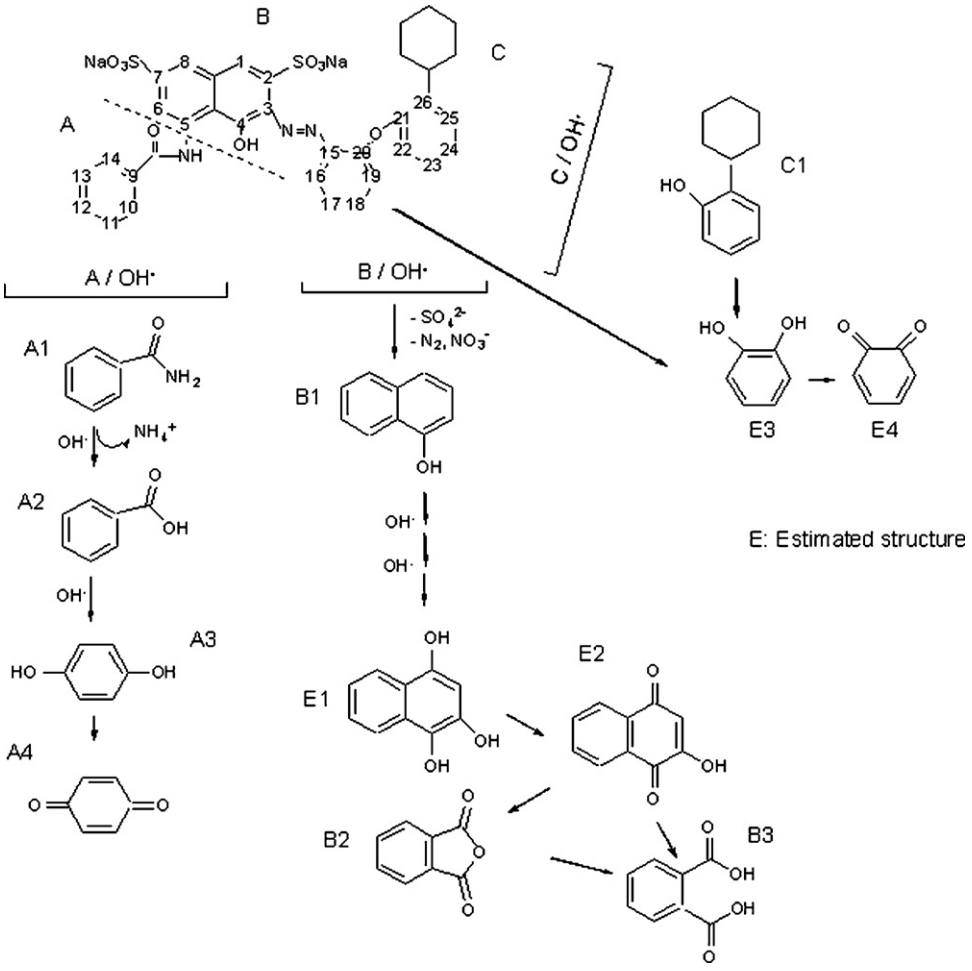

Fig. 8. GC–MS analysis of the organic intermediates of AR 274 in subcritical water (T = 175 °C, H_2O_2 = 150 mM, experiment time = 15 min).

led to the formation of 1-naphthol (**B1**) compounds. **B1** could be further oxidized to naphthalene-1,2,4-triol (**E1**) and 3-hydroxy-1,4-napthoquinone (**E2**). Compound **E2** could be converted to phthalic anhydride (**B2**) and phthalic acid (**B3**). The cleavage of the C(20)–O bond concluded to form o-cyclohexylphenol (**C1**) compounds. Catechol (**E3**) and 1,2-benzoquinone (**E4**) are other structures that are expected. For a longer duration of oxidation, all aromatic compounds would be further transformed into small molecules.

4. Conclusions

The degradation of the azo dye Acid Red 274 was carried out using H_2O_2 as oxidant in subcritical water condition. The process was optimized by using RSM based on the Box–Behnken design. The optimum values of experimental temperature, H_2O_2 concentration, and reaction time were 217 °C, 111 mM, and 60 min, respectively, where 67% TOC removal could be obtained from the proposed model. The analysis of variance showed a high coefficient of determination value (R^2 = 0.9930 and Adj-R^2 = 0.9839). The results of TOC values indicated that the subcritical water process could be used for the complete degradation of AR 274. In this way, the degradation mechanism of azo dye in subcritical water was discussed and the probable degradation pathway was deduced.

References

[1] I. Oller, S. Malato, J.A. Sánchez-Perez, Combination of advanced oxidation processes and biological treatments for wastewaters decontamination – a review, Sci. Total Environ. (2010), doi:10.1016/j.scitotenv.2010.08.061.
[2] A. Al-Kdasi, A. Idris, K. Saed, C. Teong Guan, Treatment of textile wastewater by advanced oxidation processes – a review, Global Nest. Int. J. 6 (2004) 222–230.
[3] O.Ö. Söğüt, M. Akgün, Removal of C.I. basic blue 41 from aqueous solution by supercritical water oxidation in continuous-flow reactor, J. Ind. Eng. Chem. 15 (2009) 803–808.
[4] S.D. Hosseini, F.S. Asghari, H. Yoshida, Decomposition and decoloration of synthetic dyes using hot/liquid (subcritical water), Water Res. 44 (2010) 1900–1908.
[5] E. Kuşvuran, O. Gülnaz, A. Şamil, Ö. Yildirim, Decolorization of malachite green decolorization kinetics and stoichiometry of ozone–malachite green and removal of antibacterial activity with ozonation processes, J. Hazard. Mater. 186 (2011) 133–143.
[6] X. Dong, W. Ding, X. Zang, X. Liang, Mechanism and kinetics model of degradation of synthetic dyes by UV–vis/H_2O_2/ferrioxalate complexes, Dyes and Pigments 74 (2007) 470–476.
[7] L.G. Devi, S.G. Kumar, K.M. Reddy, C. Munikrishnappa, Photo degradation of Methyl Orange an azo dye by Advanced Fenton Process using zero valent metallic iron: Influence of various reaction parameters and its degradation mechanism, J. Hazard. Mater. 164 (2009) 459–467.
[8] S. Erdemoglu, S. Karaaslan, F. Sayılkan, B. Izgi, M. Asiltürk, H. Sayılkan, F. Frimmel, Ş. Güçer, Photocatalytic degradation of Congo Red by hydrothermally synthesized nanocrystalline TiO_2 and identification of degradation products by LC–MS, J. Hazard. Mater. 155 (2008) 469–476.
[9] A. Özcan, M.A. Oturan, N. Oturan, Y. Şahin, Removal of Acid Orange 7 from water by electrochemically generated Fenton's reagent, J. Hazard. Mater. 163 (2009) 1213–1220.

[10] A. Rodríguez, G. Ovejero, M.D. Romero, C. Díaz, M. Barreiro, J. García, Catalytic wet air oxidation of textile industrial wastewater using metal supported on carbon nanofibers, J. Supercrit. Fluid. 46 (2008) 163–172.
[11] E. Chamarro, A. Marco, S. Esplugas, Use of fenton reagent to improve organic chemical biodegradability, Water Res. 35 (2001) 1047–1051.
[12] V.M. Daskalaki, E.S. Timotheatou, A. Katsaounis, D. Kalderis, Degradation of Reactive Red 120 using hydrogen peroxide in subcritical water, Desalination 274 (2011) 200–205.
[13] S.-Y. Oh, M.-K. Yoon, I.-H. Kim, Y.Y. Kim, W. Bae, Chemical extraction of arsenic from contaminated soil under subcritical conditions, Sci. Total Environ. 409 (2011) 3066–3072.
[14] M.D. Lagrega, P.L. Buckingham, J.C. Evans, Hazardous Waste Management, 2nd ed., McGraw-Hill, New York, 2000.
[15] M. Siskin, G. Brons, A.R. Katritzky, M. Balasubramanian, Aqueous organic chemistry. 1. Aquathermolysis comparison with thermolysis in the reactivity of aliphatic-compounds, Energy Fuel 4 (1990) 475–482.
[16] B. Kuhlmann, E.M. Arnett, M. Siskin, Classical organic-reactions in pure superheated water, J. Org. Chem. 59 (1994) 3098–3101.
[17] A.A. Dadkhah, A. Akgerman, Hot water extraction with in situ wet oxidation: PAHs removal from soil, J. Hazard. Mater. 93 (2002) 307–320.
[18] S.B. Hawthorne, A.J.M. Lagadec, D. Kalderis, A.V. Lilke, D.J. Miller, Pilot-scale destruction of TNT, RDX, and HMX on contaminated soils using subcritical water, Environ. Sci. Technol. 34 (2000) 3224–3228.
[19] R. Weber, S. Yoshida, K. Miwa, PCB destruction in subcritical and supercritical water-evaluation of PCDF formation and initial steps of degradation mechanisms, Environ. Sci. Technol. 36 (2002) 1839–1844.
[20] A. Kubatova, A.J.M. Lagadec, S.B. Hawthorne, Dechlorination of lindane, dieldrin, tetrachloroethane, trichloroethene, and PVC in subcritical water, Environ. Sci. Technol. 36 (2002) 1337–1343.
[21] M.A. Rauf, N. Marzouki, B.K. Körbahti, Photolytic decolorization of Rose Bengal by UV/H_2O_2 and data optimization using response surface method, J. Hazard. Mater. 159 (2008) 602–609.
[22] S.S. Moghaddam, M.R. Alavi Moghaddam, M. Arami, Response surface optimization of acid red 119 dye from simulated wastewater using Al based waterworks sludge and polyaluminium chloride as coagulant, J. Environ. Manage. 92 (2011) 1284–1291.
[23] G.E.P. Box, N.R. Draper, Response Surface, Mixtures and Ridge Analyses, 2nd ed., Wiley, USA, 2007.
[24] Y. Yang, B. Kayan, N. Bozer, B. Pate, C. Baker, A.M. Gizir, Terpene degradation and extraction from basil and oregano leaves using subcritical water, J. Chromatogr. A 1152 (2007) 262–267.
[25] Y. Yang, F. Hildebrand, Phenanthrene degradation in subcritical water, Anal. Chim. Acta 555 (2006) 364–369.
[26] F. Ay, E.C. Çatalkaya, F. Kargi, A statistical experiment design approach for advanced oxidation of Direct Red azo-dye by photo-Fenton treatment, J. Hazard. Mater. 162 (2009) 230–236.
[27] S.L.C. Ferreira, R.E. Bruns, H.S. Ferreira, G.D. Matos, J.M. David, G.C. Brando, E.G.P. da Silva, L.A. Portugal, P.S. dos Reis, A.S. Souza, W.N.L. dos Santos, Box–Behnken design: an alternative for the optimization of analytical methods, Anal. Chim. Acta 597 (2007) 179–186.
[28] M. Li, C. Feng, Z. Zhang, R. Chen, Q. Xue, C. Gao, N. Sugiura, Optimization of process parameters for electrochemical nitrate removal using Box–Behnken design, Electrochim. Acta 56 (2010) 265–270.
[29] E. Hamed, A. Sakr, Application of multiple response optimization technique to extended release formulations design, J. Control. Release 73 (2001) 329–338.
[30] A. Kumar, B. Prasad, I.M. Mishra, Optimization of process parameters for acrylonitrile removal by a low-cost adsorbent using Box–Behnken design, J. Hazard. Mater. 150 (2008) 174–182.
[31] P. Sharma, L. Singh, N. Dilbaghi, Optimization of process variables for decolorization of Disperse Yellow 211 by *Bacillus subtilis* using Box–Behnken design, J. Hazard. Mater. 164 (2009) 1024–1029.
[32] Z. Zhang, H. Zheng, Optimization for decolorization of azo dye acid green 20 by ultrasound and H_2O_2 using response surface methodology, J. Hazard. Mater. 172 (2009) 1388–1393.
[33] S.S. Moghaddam, M.R. Alavi Moghaddam, M. Arami, Coagulation/flocculation process for dye removal using sludge from water treatment plant: optimization through response surface methodology, J. Hazard. Mater. 175 (2010) 651–657.
[34] K.P. Singh, S. Gupta, A.K. Singh, S. Sinha, Optimizing adsorption of crystal violet dye from water by magnetic nanocomposite using response surface modeling approach, J. Hazard. Mater. 186 (2011) 1462–1473.
[35] N. Kannan, S.S. Balamurugan, Biosynthesis of silver nanoparticles: Parameter optimization using response surface method, Colloids Surf. B: Biointerfaces (2011), doi:10.1016/j.colsurfb.2011.05.034.
[36] A. Özer, G. Gürbüz, A. Çalımlı, B.K. Körbahti, Biosorption of copper(II) ions on *Enteromorpha prolifera*: application of response surface methodology (RSM), Chem. Eng. J. 146 (2009) 377–387.
[37] P. Sharma, L. Singh, N. Dilbaghi, Response surface methodological approach for the decolorization of simulated dye effluent using *Aspergillus fumigatus fresenius*, J. Hazard. Mater. 161 (2009) 1081–1086.
[38] M.B. Kasiri, A.R. Khataee, Photooxidative decolorization of two organic dyes with different chemical structures by UV/H_2O_2 process: experimental design, Desalination 270 (2011) 151–159.
[39] M.A. Behnajady, N. Modirshahla, H. Fathi, Kinetics of decolorization of an azo dye in UV alone and UV/H_2O_2 processes, J. Hazard. Mater. 136 (2006) 816–821.
[40] M.A. Behnajady, N. Modirshahla, Evaluation of electrical energy per order (E(EO)) with kinetic modeling on photooxidative degradation of C.I. Acid Orange 7 in a tubular continuous-flow photoreactor, Ind. Eng. Chem. Res. 45 (2006) 553–557.